Amorphous-to-crystalline transition during the early stages of thin film growth of Cr on SiO_2

Minghui Hu,[a] Suguru Noda,[b] and Hiroshi Komiyama

Department of Chemical System Engineering, University of Tokyo

7-3-1 Hongo, Bunkyo-ku, Tokyo 113-8656, Japan

The growth of sputter-deposited Cr thin films on amorphous SiO_2 during the early stages was studied using transmission electron microscopy. Amorphous three-dimensional islands were first formed, and then they grew with the continuously increasing density and slowly increasing size as the deposition proceeded. When these islands began to coalesce at a nominal film thickness of 2.3 - 3.0 nm, they abruptly crystallized into randomly oriented crystalline nuclei. The depth profile analysis by x-ray photoelectron spectroscopy indicates the existence of interfacial Cr-O interactions. After excluding the possibilities of kinetic limitation and interfacial mixing, a thermodynamic model was employed to explain the size-dependent amorphous-to-crystalline transition. Our results suggest that the interfacial-interaction-induced strain relaxation at island/substrate interfaces might

---

[a] Authors to whom correspondence should be addressed; electronic mail:

mhu@chemsys.t.u-tokyo.ac.jp

[b] Also could be addressed to; electronic mail: noda@chemsys.t.u-tokyo.ac.jp

result in the thermodynamic stabilization of substrate-supported amorphous islands below a critical size.

I. INTRODUCTION

With the continuous breakdown of sizes and the increased demand on performances for optic, electronic, and magnetic devices, the control of thin film structures during the early stages of growth is becoming increasingly significant. Many efforts have been devoted to investigations of the growth mode,[1-3] formation of crystallographic structures,[4-14] and kinetic morphology evolution of island ensembles, such as island size and density.[15-23]

Most of the research on nucleation has been conducted from the viewpoint of classical nucleation theory (CNT), which describes the vapor-liquid or liquid-solid/crystal phase transition by employing macroscopic thermodynamic concepts. It involves the existence of critical nuclei corresponding to a maximum point on the curve of the free energy change versus island size during condensation or solidification. Recently, some semiconductors,[4,5] metals,[6-8] and metal compounds[24-26] have been found to exhibit a size-dependent amorphous-to-crystalline transition during the early stages of thin film growth: at first, the amorphous islands/films are formed, subsequently evolving into the crystalline phase above the critical size of a few nanometers. It has never been clarified whether this abrupt nucleation from the amorphous phase can be explained from the CNT or not.

In total, three mechanisms might be responsible for the size-dependent amorphous-to-crystalline transition for thin film growth. They are the kinetic limitation, interfacial mixing, and thermodynamic stability. Ekinci *et al.*[6] used the kinetic model to

explain the amorphous-to-crystalline transition of 2-nm Au and Pb films deposited on Highly Orientated Pyrolytic Graphite (HOPG) at 77 K. In that model, it is supposed that adatoms initially "stick" where they land and are unable to move to equilibrium positions. On the other hand, Baji *et al.*[8] suggested the interfacial-mixing model to explain the amorphous-to-crystalline transition of 2-nm Mo layers deposited on amorphous Si at room temperature. In that model, it is assumed that the interfacial diffusion results in the formation of $MoSi_2$. Besides the above two explanations, the size-dependent difference in thermodynamic stability between amorphous and crystalline phases might also be responsible for the above transition. Such a thermodynamic model was adopted for some size-dependent structural transitions in the solid phase, such as the geometrical evolution of unsupported metal nano-clusters in the gas phase,[27] the crystalline-phase transformation of ZrO_2 on silica glass,[28,29] and the annealing-induced crystallization of amorphous Si.[30,31] However, no one has yet demonstrated or predicted its effectiveness in the size-dependent amorphous-to-crystalline transition. Some theoretical[10-12] and experimental[14,32] studies on the crystallographic structure of unsupported metal clusters show that metal clusters composed of several hundreds of atoms might be amorphous, due to the surface-contract-driven strain relaxation. However, for substrate-supported clusters formed during thin film growth, the role of interfaces in crystallographic structure formation remains unclear.

In this work, we report on evidence of the amorphous-to-crystalline transition during the early stages of thin film growth of Cr on amorphous SiO_2 using transmission electron microscopy (TEM), and discuss it from the viewpoint of thermodynamics. Our

results suggest that the amorphous phase, other than the polyhedral or crystalline phase, might be the thermodynamically stable structure for nano-sized clusters supported on amorphous substrates.

II. EXPERIMENTAL

Si(100) wafers with a thermally oxidized, 15-nm SiO_2 layer were used as substrates. They were washed using an H_2SO_4/H_2O_2 mixture. Cr was deposited at room temperature with a radio-frequency magnetron sputter system in a pure Ar atmosphere. The base pressure prior to deposition and the working pressure during the deposition were 4.0×10^{-5} and 0.8 Pa, respectively. The film growth rate during the bulk growth stage was 0.11 nm/s, which was estimated by plotting the film thickness, d_f, versus the deposition time, t_d. We define the bulk growth as the growth that occurs after the formation of continuous films. The film thickness during the bulk growth stage was measured with a TENCOR P-10 surface profiler, and during the early growth stages was measured from cross-sectional TEM (XTEM) images. To prevent thin-film structures from being destroyed during specimen preparation and TEM observations, a 10- to 15-nm SiO_2 cap layer was continually deposited onto Cr thin films without breaking the vacuum of the sputter chamber.

TEM images and selected area electron diffraction (SAED) patterns were taken using a JEOL JEM2010F operating at 200 kV. Specimens for TEM observations were prepared using conventional mechanical grinding, polishing, and dimpling, followed by Ar ion milling at an acceleration voltage of 4 keV and an incidence angle of 6°. X-ray

photoelectron spectroscopy (XPS) measurements were conducted using a PHI 1600 photoelectron spectrometer equipped with an Al *K*α source ($h\nu$ = 1486.6 eV). The emitted photoelectrons were collected at a take-off angle of 45° from a 3×3 mm^2 area sputter-etched with a 4 keV argon-ion beam. There was no detectable charge-up judged from the constant position of the photoelectron peaks during analysis. After subtracting the spectral background using the Shirley algorithm,[33] the Cr $2p_{3/2}$ peak fitting was implemented by using a mixed Gaussian/Lorentzian curve with an exponential tail component at the high binding energy side.[34]

III. RESULTS

A. Formation and evolution of crystallographic structure of Cr islands/films

XTEM observations show the growth mode of Cr thin films on SiO_2, and the structural evolution with deposition time. As shown in Fig. 1, XTEM images of Cr thin films for $2 \leq t_d \leq 35$ s exhibit a sudden variation in the thin-film structure between t_d = 10 and 20 s. The contrast of Cr thin films for $2 \leq t_d \leq 10$ s [Figs. 1(a)-1(d)] was uniform, whereas that for $20 \leq t_d \leq 35$ s [Figs. 1(e) and 1(f)] depended on the position of the thin films. This can be seen more clearly in high-resolution cross-sectional TEM (HRXTEM) images of Cr thin films at t_d = 2 and 20 s, as shown in Fig. 2. At t_d = 2 s [Fig. 2(a)], isolated 3D islands were formed, indicative of the 3D-island growth mode. Moreover, these islands did not exhibit a lattice structure but an amorphous structure. The amorphous feature remained at least until t_d = 10 s, whereas the lattice structure first appeared in the Cr film at t_d = 20 s [Fig. 2(b)]. This demonstrates that the

amorphous islands were formed first, and changed into the crystalline phase as the deposition proceeded.

In-plane TEM observations also provide explicit evidence of the formation and evolution of crystallographic structures. Fig. 3 shows plan-view TEM images of Cr thin films for $2 \leq t_d \leq 35$ s, as well as the corresponding SAED images. The SAED images of Cr thin films for $2 \leq t_d \leq 10$ s [Figs. 3(a)-3(d)] exhibited a halo pattern, which demonstrates that the Cr 3D islands were amorphous. However, Cr thin films for $20 \leq t_d \leq 35$ s [Figs. 3(e) and 3(f)] exhibited multi-ring patterns, corresponding to (110) and (200) planes of the body-centered cubic (bcc) polycrystal structure, respectively. This change in SAED patterns unequivocally indicates the abrupt amorphous-to-crystalline transition for Cr islands/films at the deposition time, $10 < t_d < 20$ s.

To further investigate the growth of these crystalline nuclei, we observed the crystalline structure of Cr thin films for $t_d > 35$ s. The XTEM image of the Cr film at $t_d = 50$ s [Fig. 4(a)] showed some domains with the non-uniform contrast. Among the corresponding high-resolution TEM (HRTEM) images of different areas of this thin film, as indicated by arrows, Figs. 4(b) and 4(c) exhibited the (110) lattice plane of bcc Cr with the same orientation, implying that they were from the same single-crystalline grain. However, different domains, as shown in Figs. 4(d) and 4(e), exhibited the (110) lattice plane with different orientations. This suggests that one domain corresponds to one single-crystalline grain, and that these grains/nuclei are planular and elongated in shape. As shown in Fig. 5, plan-view HRTEM images also manifest the same results.

Besides the shape of crystalline nuclei, it is also interesting to know their crystallographic orientation. The SAED pattern shown in Fig. 5 suggests that Cr grains might have a random crystalline orientation. It is easy to distinguish that the strength sequence of the diffraction rings was (110) > (211) > (200). Meanwhile, the diffraction strengths of the (110), (211), and (200) planes of bcc Cr are 100%, 30%, and 16%, respectively, according to JCPDS card No. 6-0694. Their accordance supports the conclusion that crystallized Cr thin films are polycrystals composed of grains randomly orientated in both the in-plane and out-of-plane directions, most of which have a planular and elongated shape in the in-plane direction.

B. Time-dependent evolution of Cr island size and density

TEM observations provide evidence of the amorphous-to-crystalline transition that occurred at the deposition time, $10 < t_d < 20$ s, and suggest the subsequent formation of randomly orientated crystalline nuclei. In order to comprehensively understand the above phenomena, we investigated the growth characteristics of Cr island ensembles, such as island size and density.

As shown in Fig. 6, the nominal film thickness, d_f, did not increase linearly with deposition time, t_d, during the early growth stages. At the beginning of deposition, d_f, quickly increased to 1.5 nm at $t_d = 2$ s, followed by a slow increase to 3.2 nm at $t_d = 35$ s. After that, the film growth rate approached the bulk growth rate of 0.11 nm/s. As explained in the following, this change in nominal film thickness is closely related to the evolution of island size and density.

As seen from plan-view TEM images, the Cr thin films for $2 \leq t_d \leq 10$ s [Figs. 3(a)-3(d)] were discontinuous, and composed of isolated 3D islands. Because the nominal film thickness observed in the XTEM images is identical to the island height, the slowdown in film thickening for $2 \leq t_d \leq 35$ s means a slow increase in island height. Measured from the cross-sectional and plan-view TEM images [Figs. 1 and 3], the mean island height, H, increased from 1.5 to 2.3 nm when t_d increased from 2 to 10 s. Concomitantly, the mean island diameter, D, increased from 2.5 to 3 nm. It is noteworthy that H is smaller than D during the stages of island growth [Fig. 7(a)], which implies that Cr islands on SiO_2 surfaces have a spherical-cap shape. Their contact angle throughout the deposition time from 2 to 10 s, θ, was calculated to be approximately 110$\pm$10°, according to the following equation:

$$\cos(\theta) = \frac{\frac{D}{2} - H}{\frac{D}{2}} \tag{1}$$

Furthermore, the Cr/SiO_2 interfacial energy was estimated to be approximately 1.40$\pm$0.4 J/m^2, since the surface energies of SiO_2 and Cr are 0.62[35] and 2.30[36] J/m^2, respectively.

The 3D-island density, N_d, was directly counted from plan-view TEM images shown in Figs. 3(a)-3(d), and its variation against the deposition time is plotted in Fig. 7(b). N_d increased threefold from 2×10^{16} /m^2 at $t_d = 2$ s to 6×10^{16} /m^2 at $t_d = 10$ s. It is reasonable that the island distance should decrease to such an extent that these islands begin to coalesce and evolve into an island-network structure. This is due to the continuous

increase in island density rather than the slow increase in island size. In the next section, this island-growth process is discussed in more detail.

After quantitatively evaluating the island shape, size, and density, we estimated the sticking coefficient of Cr on SiO_2 substrates by comparing deposited film amounts during the early stage with the bulk growth stage. The deposited film volume, V, was calculated from the island geometry, size, and density, according to the following equations:

$$V = v \times N_D \tag{2}$$

$$v = \frac{4}{3}\pi\left(\frac{D}{2}\right)^3 \alpha(\theta) \tag{3}$$

$$\alpha(\theta) = \frac{2 - 3\cos\theta + \cos^3\theta}{4} \tag{4}$$

As shown in Fig. 8, before island coalescence, V was proportional to t_d at a constant rate similar to that during the bulk growth stage. In other words, Cr atoms stick to SiO_2 substrates with almost the same probability as to Cr itself.

In summary, Cr 3D islands with the spherical-cap shape have an estimated contact angle of approximately $110 \pm 10^\circ$. Island coalescence occurred as a result of the continuous increase in island density rather than the slow increase in island size. The amount of deposited thin films linearly increased with deposition time throughout the early and bulk stages, which means the almost same sticking coefficient for Cr on SiO_2 as that on Cr.

C. Analysis of Cr/SiO_2 interfaces

The thin film growth during the early stages greatly depends on interfacial interactions. We analyzed the interface state between Cr thin films and SiO_2 substrates using TEM and XPS. First, the physical state of Cr/SiO_2 interfaces was directly observed using TEM. Two facts are seen from the HRXTEM image of the Cr thin film at t_d = 50 s [Fig. 9]. One is the absence of amorphous Cr structures remaining on the SiO_2 surface. The other is the presence of Cr lattice structures stretching to the SiO_2 surface. Because a clear boundary existed between the crystalline Cr thin film and the amorphous SiO_2 substrate, we concluded that no interfacial mixing occurred between Cr thin films and SiO_2 substrates. That is, the interfacial diffusion, even if occurring below the HRXTEM-detected level, does not affect the abrupt crystallization of Cr thin films at the nominal thickness of 2.3 - 3.0 nm.

Then, the chemical state of Cr at Cr/SiO_2 interfaces was investigated using XPS. The elemental composition in depth for the 25-nm Cr thin film with a structure of $Cr/SiO_2/Si$ is shown in Fig. 10. Exposure to air causes the oxidization of the thin film surface. Below that oxide layer, the thin film composition is homogeneous until $t_e < 12$ min. However, during $12 \leq t_e \leq 16$ min, the strength of the Cr signal linearly decreased, whereas that of the C signal, which originates from the pollution of the SiO_2 surface, first increased and then decreased back to its original level. For $t_e > 12$ min, the strength of the Cr signal began to decrease nonlinearly with a long tail due to the limited depth resolution. Therefore, the interfacial Cr thin film is located within the span between $12 \leq t_e \leq 16$ min in the XPS depth profile.

Cr $2p_{3/2}$ peaks between $12 \leq t_e \leq 16$ min were decomposed into 574.6 and 576.2 eV components [Fig. 11], corresponding to metallic (Cr^0) and oxidized ($Cr^{\delta+}$) species, respectively.[34,37] A small amount of $Cr^{\delta+}$ in the Cr thin film might result from the oxidation by the residual oxygen in the sputter chamber. Both of the peak intensities of Cr^0 and $Cr^{\delta+}$ were constant in the bulk films, whereas at the Cr/SiO_2 interfaces, the former decreased and the latter increased [Fig. 12]. Quantitative analysis indicates that the ratio of $Cr^{\delta+}$ to the total Cr atoms at Cr/SiO_2 interfaces increased up to about 10% after subtracting the intrinsic amount of residual $Cr^{\delta+}$ in bulk Cr films. Since the mean escape depth of Cr $2p_{3/2}$ photoelectrons is less than 2 nm,[34,38] the amount of $Cr^{\delta+}$ at the Cr/SiO_2 interfaces is probably as little as one monolayer, implying that Cr-O interactions are limited within a single contact layer between Cr and SiO_2.

IV. DISCUSSION

The most significant growth characteristic of sputter-deposited Cr thin films on amorphous SiO_2 during the early stages is the abrupt amorphous-to-crystalline transition that occurred at the deposition time, $10 < t_d < 20$ s, i.e., at the nominal film thickness, $2.3 < d_f < 3.0$ nm. These amorphous 3D-islands seem to have a spherical-cap shape with an estimated contact angle of approximately $110 \pm 10°$ that is constant throughout the island growth stages for $2 \leq t_d \leq 10$ s. The island density increased continuously and their sizes increased slowly. When these islands began to coalesce, they abruptly crystallized from amorphous islands/films, followed by the formation of randomly orientated crystalline nuclei. These crystalline nuclei further evolved into planular,

elongated grains in the in-plane direction.

As elucidated in the introductory section, three mechanisms might account for the size-dependent amorphous-to-crystalline transition. First, we assume that the formation of amorphous islands before 10 s deposition and the subsequent crystallization between 10 and 20 s deposition are due to kinetic limitations, as in the cases of the formation of unstable[6] (frozen) or metastable[39] (Ostwald step rule) phases. Accordingly, the kinetic lifetime of amorphous islands should not exceed 20 s at the substrate temperature (possibly < 100 ˚C) under sputter conditions. It is noteworthy that all the specimens were heated at 150 - 180 ˚C for 10 - 30 min during the specimen preparation before TEM observations. The existence of amorphous islands shown in the TEM images contradicts with their expected kinetic lifetime. Therefore, the kinetic limitation can not be the factor that determines the crystallographic evolution of Cr islands. On the other hand, the existence of sharp Cr/SiO_2 interfaces, together with the XPS results, rules out the possibility of the formation of a thermodynamically stable mixed Cr/O interlayer, followed by the crystallization of subsequent Cr thin films above that interlayer. Therefore, the thermodynamic reason is left as the only factor that might determine the size-dependent crystallization of amorphous Cr islands/films.

Let's follow the approach adopted in the CNT and consider the free energy change, ΔG_{a-c}, of an amorphous island during its crystallization. It involves three contributions: volume, surface, and interface. Assuming that the island shape (spherical-cap) and the contact angle remain constant before and after crystallization, ΔG_{a-c} can be expressed as follows,

$$\Delta G_{a-c} = \frac{4}{3}\pi R^3 \alpha(\theta) \Delta G^{v}{}_{a-c} + 2\pi R^2 (1-\cos\theta) \Delta\gamma^{s}{}_{a-c} + \pi R^2 \sin^2\theta\, \Delta\gamma^{i}{}_{a-c} \tag{5}$$

$$\alpha(\theta) = \frac{2 - 3\cos\theta + \cos^3\theta}{4} \tag{6}$$

where $\Delta G^{v}{}_{a-c}$, $\Delta\gamma^{s}{}_{a-c}$, and $\Delta\gamma^{i}{}_{a-c}$ are the free energy changes in volume per unit volume, surface per unit area, and interface per unit area, respectively; and R is the island radius. The volume term is proportional to the cube of the island size, whereas the surface/interface terms are proportional to the square of the island size. Under our experimental conditions, the bulk crystalline phase is apparently more stable than the bulk amorphous phase, i.e., the volume term is negative. If the sum of the surface and interface terms is positive, ΔG_{a-c} will first increase with island size, and then reach a maximum value at a critical point, R^*, as indicated in Eq. (7):

$$\frac{\partial \Delta G_{a-c}}{\partial R} = 0\ , \quad R^* = \frac{(1-\cos\theta)\Delta\gamma^{s}{}_{a-c} + \frac{1}{2}\sin^2\theta\,\Delta\gamma^{i}{}_{a-c}}{-\alpha(\theta)\Delta G^{v}{}_{a-c}} \tag{7}$$

After that, ΔG_{a-c} will decrease with island size, and become negative upon another critical island size, R^{**}, as indicated in Eq. (8):

$$\Delta G_{a-c} = 0\ , \quad R^{**} = \frac{\frac{3}{2}(1-\cos\theta)\Delta\gamma^{s}{}_{a-c} + \frac{3}{4}\sin^2\theta\,\Delta\gamma^{i}{}_{a-c}}{-\alpha(\theta)\Delta G^{v}{}_{a-c}} \tag{8}$$

Then, let's consider the formation of a crystalline nucleus with a size of r in an amorphous island with a size of R. When $r > R^*$, then $\frac{\partial \Delta G_{a-c}}{\partial R} < 0$; when $r > R^{**}$, then $\Delta G_{a-c} < 0$. That is, R^* is the critical size for the inside crystalline nucleus to tend to grow larger by incorporating surrounding atoms in the amorphous island, and R^{**} is the critical size for this once formed nucleus to exist stably, i.e., crystallize. For the

crystallization of an amorphous island of $R < R^{**}$, the size of inside crystalline nucleus can not exceed R^{**}, which means that this unstable nucleus will return into stable amorphous phase. Only an amorphous island of $R > R^{**}$ can irreversibly change into a crystalline nuclei. In other words, the amorphous-to-crystalline transition is thermodynamically permitted only for amorphous islands larger than R^{**}. This critical size, R^{**}, might correspond to the experimentally observed Cr island size at the nominal film thickness of 2.3 - 3.0 nm.

The above thermodynamic model can describe the amorphous-to-crystalline transition during the early stages of thin film growth of Cr on SiO_2. Nevertheless, two key issues remain unresolved. One is whether the sum of the free energy changes of surface and interface for Cr islands could be positive. The other is why the crystallization from the amorphous phase abruptly occurred at the very deposition time, $10 < t_d < 20$ s, i.e., at the very nominal film thickness, $2.3 < d_f < 3.0$ nm.

The first question is related to whether the surface of Cr islands in the amorphous phase is more stable than that in the crystalline phase, and whether the amorphous-Cr/amorphous-SiO_2 interface is more stable than the crystalline-Cr/amorphous-SiO_2 interface. Some theoretical calculations have predicted that for unsupported metal clusters, amorphous-like disordered structures might be more stable than ordered structures due to the surface-contract-driven strain relaxation.[10-12] However, the role of interfaces in the formation of crystallographic phases for small clusters supported on a substrate has seldom been investigated. We believe that the interface state affects the stability of the crystallographic phase more than the surface

state, because interfacial atoms directly contact the uppermost naked substrate atoms, whereas surface atoms only contact either vacuum or inert gas.

Here, we give a qualitative description for explaining the interfacial-interaction-induced strain relaxation at island/substrate interfaces. If we extend the concept of misfit out of the epitaxy, the strain induced by the difference in interfacial-atom distance, i.e, by the attraction and repulsion between substrate and island atoms, also exists in the case of non-epitaxy, such as amorphous/amorphous or crystalline/amorphous interfaces. For bulk materials, amorphous phases usually have a lower Young's modulus than crystalline phases,[40-42] because atoms in amorphous phases are free to deform. Similarly, the strain of thin film atoms at amorphous/amorphous interfaces can be relieved more easily than that at crystalline/amorphous interfaces. The strain relaxation helps decrease the interfacial energy, i.e., amorphous substrates can stabilize supported amorphous islands.

Accordingly, the sum of the surface/interface terms in the expression of ΔG_{a-c} for Cr islands on amorphous SiO_2 might be positive, which counteracts with the negative volume term, leading to the existence of the critical size, R^{**}, for amorphous islands to crystallize. Of course, the above model remains to be demonstrated by further quantitative evaluation. It should be pointed that, in fact, two SiO_2/Cr interfaces existed for our TEM specimens with the cap-SiO_2/Cr/substrate-SiO_2/Si structure, which might enlarge the critical crystallization size, but can by no means eliminate the crystallographic transition itself.

The second question can be answered by a comprehensive consideration of other growth characteristics of Cr thin films during the early stages. Cr islands were continuously formed, and they grew without migration. This is different from the island-migration-dominated growth for weak-interfacial-interactions systems. For that growth, islands have a high mobility on substrate surfaces, and they migrate and coalesce with neighbor islands, resulting in a drastic decrease in island density.[18,19,22] Because the Cr-O interactions at Cr/SiO_2 interfaces decrease the mobility of Cr islands, these islands "statically" grow where they are formed by incorporating incident atoms or diffusing adatoms. For this adatom-diffusion-dominated growth, the change in island size has the feature that the radius of small islands increases faster than that of large ones,[21] which agrees with our experimental results. However, for the migration-dominated growth, the island size increases quickly due to the migration-induced coalescence.[18,19,22] Therefore, for Cr thin films on SiO_2, islands begin to coalesce only as a result of the continuously increasing island density rather than the slowly increasing island size.

Then, for the adatom-diffusion-dominated growth, the size of an amorphous island will exceed the threshold of crystalline nucleation in either of the following two ways. One is the slowly increasing island size through the incorporation of Cr atoms/adatoms. The other is the abruptly increasing island size through the growth-induced coalescence. Both of them can only occur at later stages of Cr island growth, which causes the amorphous-to-crystalline transition observable at the experimental time/spatial scale. However, for the island-migration-dominated growth, the rapidly increasing island size, due to the migration-induced coalescence, makes it difficult to observe crystalline

nucleation of initially formed amorphous islands.[9,13] It is obvious that the amorphous-to-crystalline transition is closely associated with the mobility of Cr adatoms/islands mainly determined by interfacial interactions. In our case, the coincidence of the onset of crystalline nucleation of amorphous islands and the growth-induced coalescence indicates that the crystallographic transition is more likely triggered by island coalescence. As a summary, the continuous increase in island density and the slow increase in island size due to the low mobility of Cr islands explains why the amorphous-to-crystalline transition occurred at the very deposition time, $10 < t_d < 20$ s.

TEM observations indicate that randomly orientated nuclei were formed during the crystallization, and that they evolved into planular, elongated grains in the in-plane direction. Usually, epitaxy or surface/interface energy minimization results in the preferential orientation of islands/films in the out-of-plane direction.[43] For our case, the experimental results can be understood as follows. Crystalline nucleation occurs inside amorphous domains formed during island coalescence. It is reasonable to think that crystalline nuclei are surrounded by amorphous structures of those domains. Then, surface/interfacial energies of crystalline nuclei are independent of their crystalline orientation. Therefore, the amorphous-to-crystalline transition gives rise to the formation of crystalline nuclei with random orientation. These nuclei further grow in the amorphous domains along the in-plane direction, which results in the formation of planular, elongated grains.

Our study indicates the importance of interfacial interactions in the structural evolution of nano-sized islands with a large surface/interface-to-volume ratio, and the necessity for a quantitative evaluation of the strain relaxation between islands/thin films and amorphous substrates. By far, most experimental and theoretical studies on interfacial interactions are focused in the case of thin film growth on crystalline substrates. On these so-called well-defined substrates, besides the chemical interactions, the interface strain is also one form of interfacial interactions, which can be quantitatively evaluated by the misfit between thin films and substrates.[44] Although thin film growth on amorphous substrates should also have similar situations, how to define and evaluate the misfit, strain, and interfacial interactions for these cases remains unresolved. We expect more efforts to be devoted to the issues that have been exhibited in this work.

V. CONCLUSIONS

We have investigated the structural evolution of Cr 3D islands on amorphous SiO_2 and found the amorphous-to-crystalline transition at the nominal film thickness of 2.3 - 3.0 nm when islands began to coalesce due to the increase in island density. The Cr-O interactions at Cr/SiO_2 interfaces were demonstrated by the increased amount of weakly oxidized Cr component at Cr/SiO_2 interfaces, which is consistent with the low mobility of Cr islands and the high sticking coefficient of Cr atoms. The thermodynamic model was employed to explain the size-dependent crystallographic transition. For the amorphous-to-crystalline transition of Cr islands below a critical size on amorphous SiO_2, the sum of free energy changes of island surface and interface, especially the latter,

might have a larger contribution to the total free energy than the free energy change of island volume. It is reasonable that amorphous/amorphous interfaces have a lower energy than crystalline/amorphous interfaces, possibly because of the difference in the interfacial-interaction-induced strain relaxation for amorphous and crystalline islands. This study indicates the necessity for a quantitative evaluation of interfacial interactions, especially strain relaxation, between islands/thin films and amorphous substrates.

ACKNOWLEDGEMENTS

This work was financially supported, in part, by the New Energy and Industrial Technology Development Organization (NEDO)'s "Nanotechnology Program - Systemization of Nanotechnology Materials Program Results Project", of the Ministry of Economy, Trade, and Industry (METI), and by the Japan Society for the Promotion of Science (JSPS)'s "Grant-in-Aid for Creative Scientific Research - Establishment of Networked Knowledge System with Structured Knowledge for Future Scientific Frontier Project", of the Ministry of Education, Culture, Sports, Science and Technology (MEXT), Japan. We thank Mr. Shinichi Nakamura (Corporate Research and Development Center, Toshiba Corporation) for his technical support and helpful discussions about TEM analysis.

Figure captions

Fig. 1. XTEM images of Cr thin films on SiO_2 at deposition times of t_d = (a) 2, (b) 5, (c) 8, (d) 10, (e) 20, and (f) 35 s.

Fig. 2. HRXTEM images of Cr thin films on SiO_2 at deposition times of t_d = (a) 2 and (b) 20 s.

Fig. 3. Plan-view TEM images of Cr thin films on SiO_2 at deposition times of t_d = (a) 2, (b) 5, (c) 8, (d) 10, (e) 20, and (f) 35 s, as well as corresponding SAED patterns.

Fig. 4. XTEM image of Cr thin films on SiO_2 at t_d = 50 s, and the corresponding HRXTEM images of selected positions from 1 to 4. The lattice constant of the Cr (110) plane is 0.204 nm.

Fig. 5. Plan-view TEM images and SAED patterns of Cr thin film on SiO_2 at t_d = 50 s, and the corresponding HRXTEM images of selected positions from 1 to 4. The lattice constant of the Cr (110) plane is 0.204 nm.

Fig. 6. Nominal film thickness, d_f, versus deposition time, t_d, during the early (square symbol) and bulk (dotted line) growth stages.

Fig. 7. Average island size (height, H, and diameter, D), and island density, N_d, versus deposition time, t_d.

Fig. 8. Deposited thin-film volume, V, versus deposition time, t_d, during the early (square symbol) and bulk (dotted line) growth stages.

Fig. 9. HRXTEM image of Cr thin film on SiO_2 at t_d = 50 s, showing the lattice structure extended out to the SiO_2 surface.

Fig. 10. XPS depth profile of 25-nm Cr thin film on SiO_2.

Fig. 11. XPS spectra of Cr $2p_{3/2}$ (a) in bulk thin film and (b) at Cr/SiO_2 interfaces.

Fig. 12. Peak intensities of Cr^0 $2p_{3/2}$ and $Cr^{\delta+}$ $2p_{3/2}$ peaks versus sputter-etching time.

References

[1]V. Musolino, A. Dal Corso, and A. Selloni, Phys. Rev. Lett. **83**, 2761 (1999).

[2]M. Hu, S. Noda, and H. Komiyama, Surf. Sci. **513**, 530 (2002).

[3]D. Fuks, S. Dorfman, Y. F. Zhukovskii, E. A. Kotomin, and A. M. Stoneham, Surf. Sci. **499**, 24 (2002).

[4]G. Fuchs, P. Melinon, S. F. Aires, M. Treilleux, B. Cabaud, and A. Hoareau, Phys. Rev. B **44**, 3926 (1991).

[5]K. Tanaka, S. Iwama, and K. Mihama, Jpn. J. Appl. Phys. **37**, L669 (1998).

[6]K. L. Ekinci and J. M. Valles Jr, Acta Mater. **46**, 4549 (1998).

[7]D. L. Windt, S. V. Christensen, W. W. Craig, C. Hailey, F. A. Harrison, M. Jimenez-Garate, R. Kalyanaraman, and P. H. Mao, J. Appl. Phys. **88**, 460 (2000).

[8]S. Bajt, D. G. Steams, and P. A. Kearney, J. Appl. Phys. **90**, 1017 (2001).

[9]W. Krakow, M. Jose-Yacaman, and J. L. Aragon, Phys. Rev. B **49**, 10591 (1994).

[10]J. M. Soler, M. R. Beltran, K. Michaelian, I. L. Garzon, P. Ordejon, D. Sanchez-Portal, and E. Artacho, Phys. Rev. B **61**, 5771 (2000).

[11]I. L. Garzon, K. Michaelian, M. R. Beltran, A. Posada-Amarillas, P. Ordejon, E. Artacho, D. Sanchez-Portal, and J. M. Soler, Phys. Rev. Lett. **81**, 1600 (1998).

[12]A. Taneda, T. Shimizu, and Y. Kawazoe, J. Phys.: Condens. Matter. **13**, L305 (2001).

[13]K. Kizuka and N. Tanaka, Phys. Rev. B **56**, R10079 (1997).

[14]M. Jose-Yacaman, M. Marin-Almazo, and J. A. Ascencio, J. Mol. Catal. A **173**, 61 (2001).

[15]A. A. Schmidt, H. Eggers, K. Herwig, and R. Anton, Surf. Sci. **349**, 301 (1996).

[16]T. I. Kamins, E. C. Carr, R. S. Williams, and S. J. Rosner, J. Appl. Phys. **81**, 211 (1997).

[17]F. M. Ross, J. Tersoff, and R. M. Tromp, Phys. Rev. Lett. **80**, 984 (1998).

[18]H. Shirakawa and H. Komiyama, J. Nanoparticle Research **1**, 17 (1999).

[19]M. Hu, S. Noda, Y. Tsuji, T. Okubo, Y. Yamaguchi, and H. Komiyama, J. Vac. Sci. Technol. A **20**, 589 (2002).

[20]J. G. Amar, M. N. Popescu, and F. Family, Surf. Sci. **491**, 239 (2001).

[21]L.-H. Chen, C.-Y. Chen, and Y.-L. Lee, Surf. Sci. **429**, 150 (2000).

[22]J. M. Zuo and B. Q. Li, Phys. Rev. Lett. **88**, 2555021 (2002).

[23]V. Dureuil, C. Ricolleau, M. Gandais, C. Grigis, J. P. Lacharme, and A. Naudon, J. Crystal Growth **233**, 737 (2001).

[24]Y.-J. Yong, J.-Y. Lee, H. S. Kim, and J. Y. Lee, Appl. Phys. Lett. **71**, 1489 (1997).

[25]T. Q. Li, S. Noda, Y. Tsuji, T. Ohsawa, and H. Komiyama, J. Vac. Sci. Technol. A **20**, 583 (2002).

[26]J. H. Choi, J. Y. Lee, and J. H. Kim, Thin Solid Films **384**, 166 (2001).

[27]J. P. K. Doye and F. Calvo, J. Chem. Phys. **116**, 8307 (2002).

[28]C. R. Aita, M. D. Wiggins, R. Whig, C. M. Scanlan, and M. Gajdardziska-Josifovska, J. Appl. Phys. **79**, 1176 (1995).

[29]T. Chraska, A. H. King, and C. C. Berndt, Mater. Sci. Eng. A **286**, 169 (2000).

[30]Y. Wakayama, T. Tagami, and S. Tanaka, Thin Solid Films **350**, 300 (1999).

[31]G. F. Grom et al., Nature **407**, 358 (2000).

[32]A. I. Frenkel, C. W. Hills, and R. G. Nuzzo, J. Phys. Chem. B **105**, 12689 (2001).

[33]D. A. Shirley, Phys. Rev. B **135**, 4709 (1972).

[34]V. Maurice, S. Cadot, and P. Marcus, Surf. Sci. **458**, 195 (2000).

[35]S. H. Overbury, P. A. Bertrand, and G. A. Somorjai, Chem. Rev. **75**, 547 (1975).

[36]W. R. Tyson and W. A. Miller, Surf. Sci. **62**, 267 (1977).

[37]A. M. Salvi, J. E. Castle, J. F. Watts, and E. Desimoni, Appl. Surf. Sci. **90**, 333 (1995).

[38]M. P. Seah and W. A. Dench, Surf. Interface Anal. **1**, 2 (1979).

[39]P. R. ten Wolde and D. Frenkel, Phys. Chem. Chem. Phys. **1**, 2191 (1999).

[40]S. M. M. Ramos, B. Canut, L. Gea, P. Thevenard, M. Bauer, Y. Maheo, P. Kapsa, and J. L. Loubet, J. Mater. Sci. **7**, 178 (1992).

[41]P. Hess, Appl. Surf. Sci. **106**, 429 (1996).

[42]T. Hartmanna et al., Nucl. Instrum. Meth. B **141**, 398 (1998).

[43]C. V. Thompson and R. Carel, Mater. Sci. Eng. B **32**, 211 (1995).

[44]W. D. Nix, Metall. Trans. A **20**, 2217 (1989).

Fig. 1

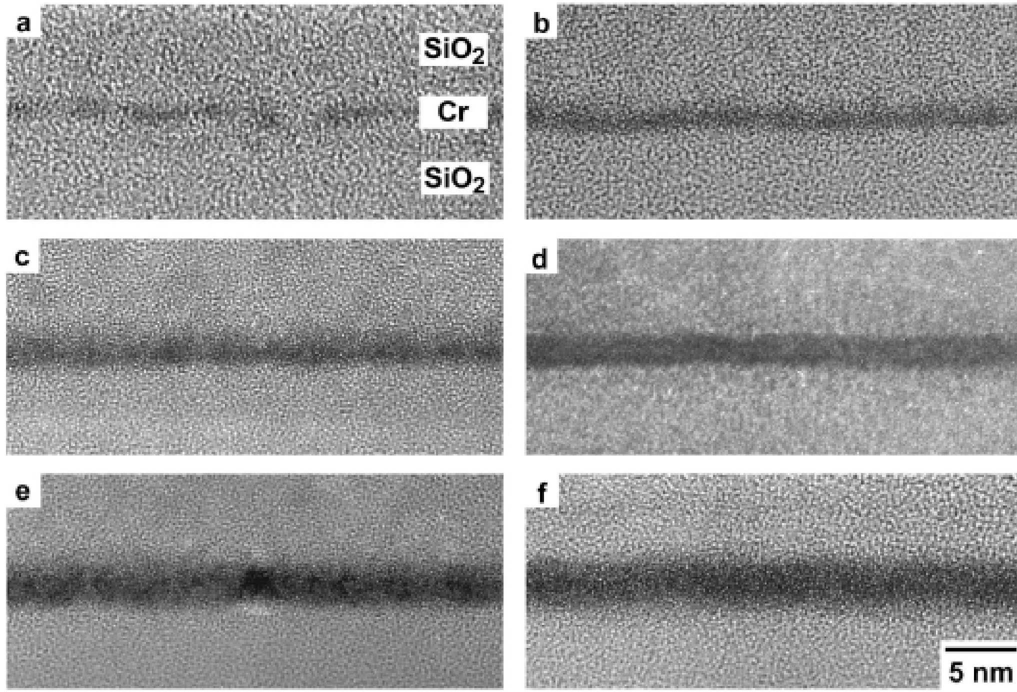

Fig. 2

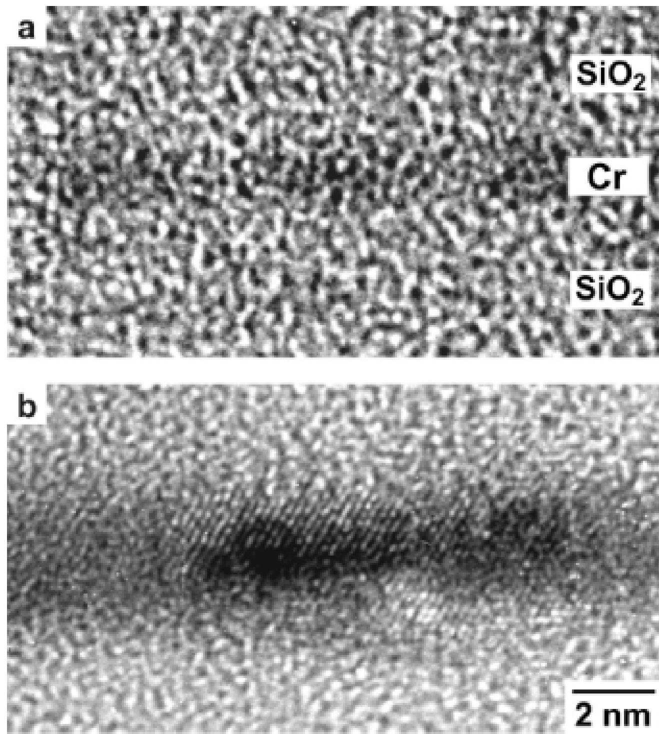

Fig. 3

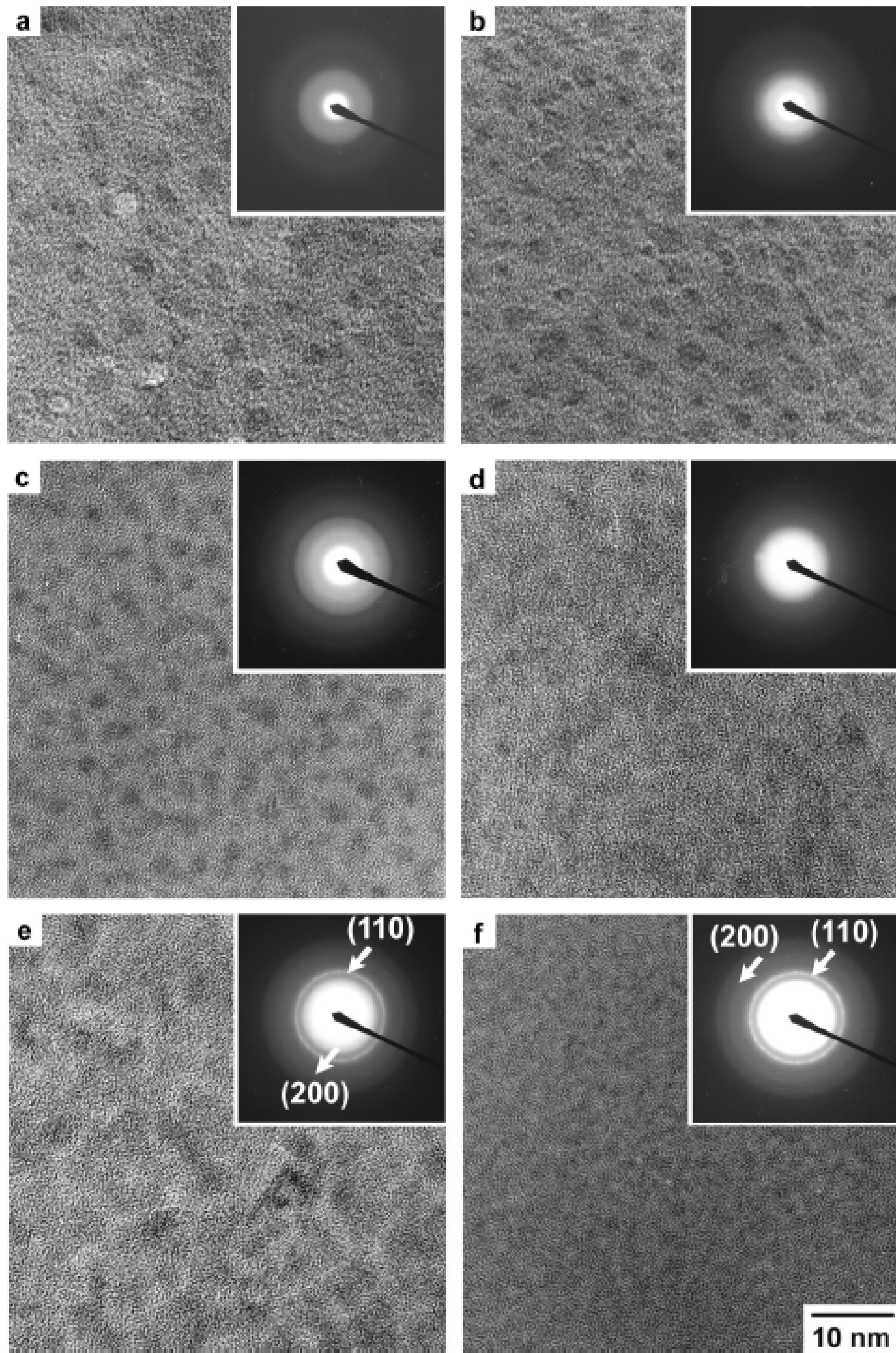

Fig. 4

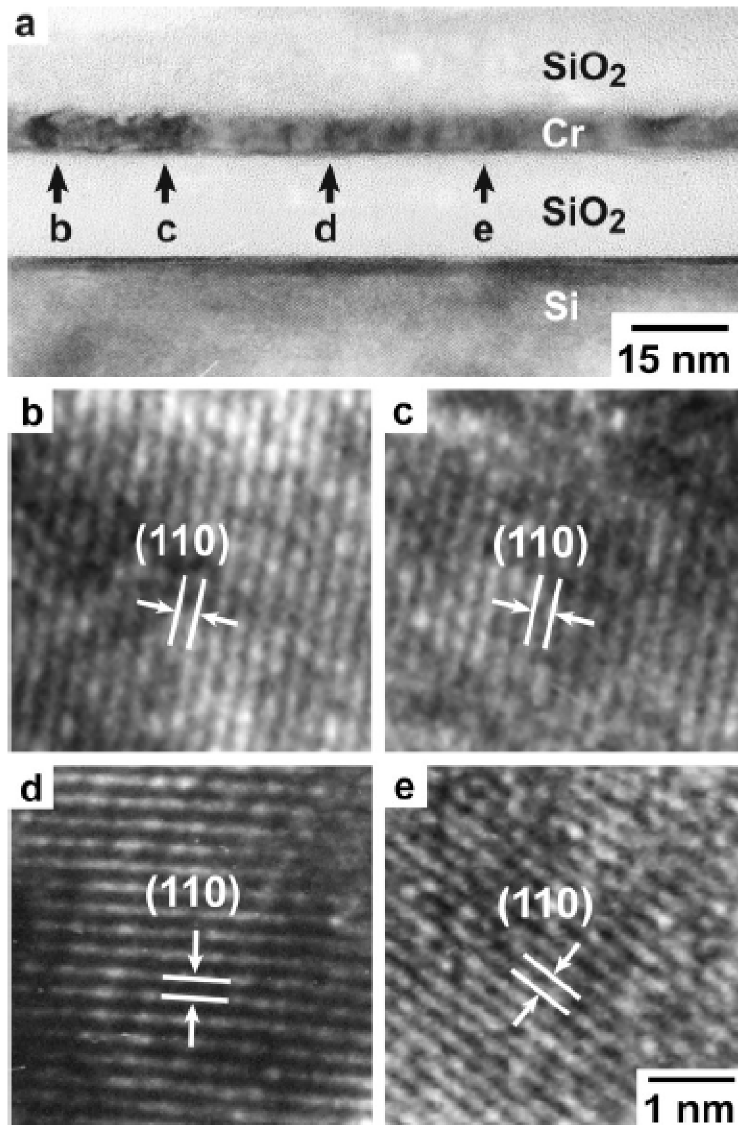

Fig. 5

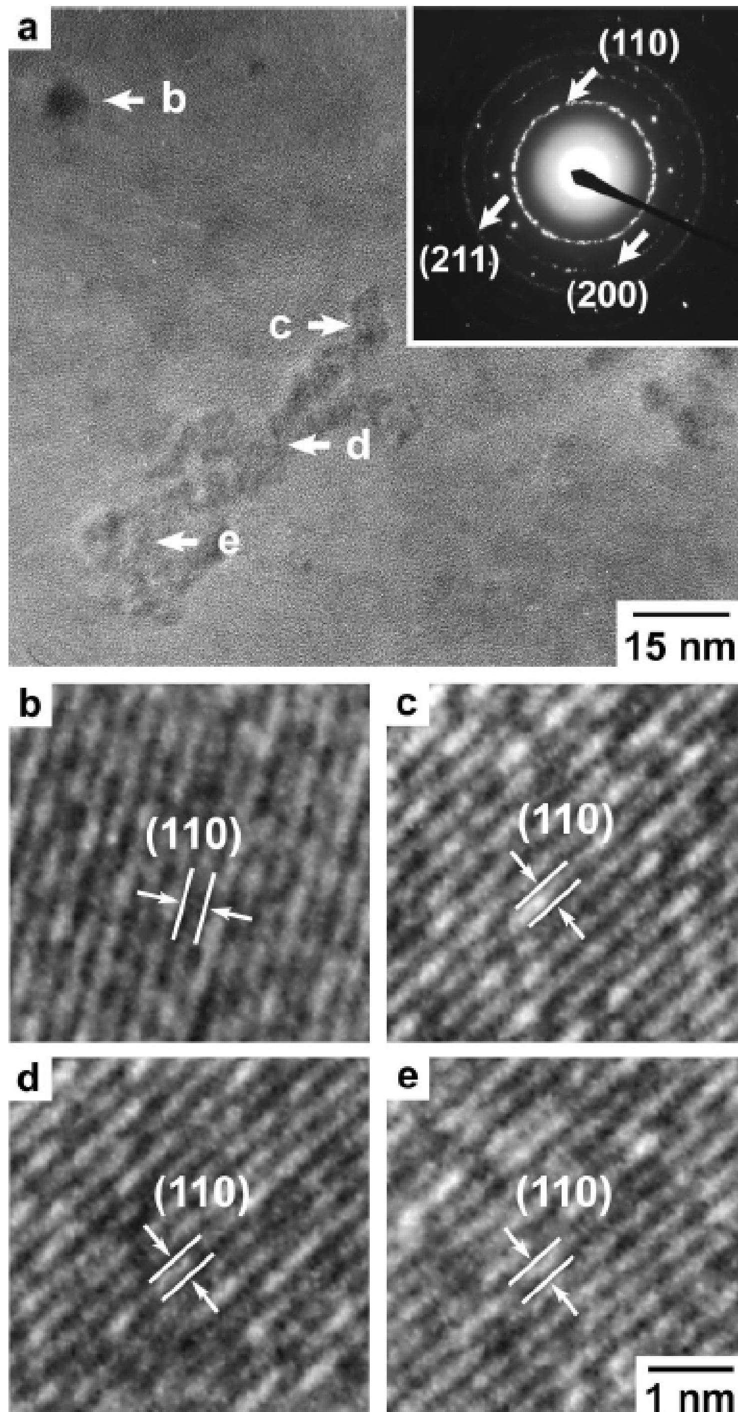

Fig. 6

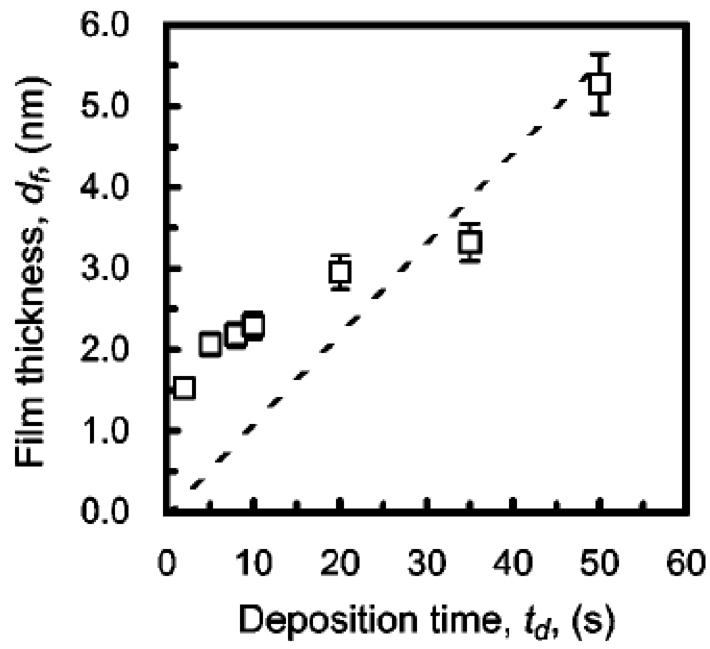

Fig. 7

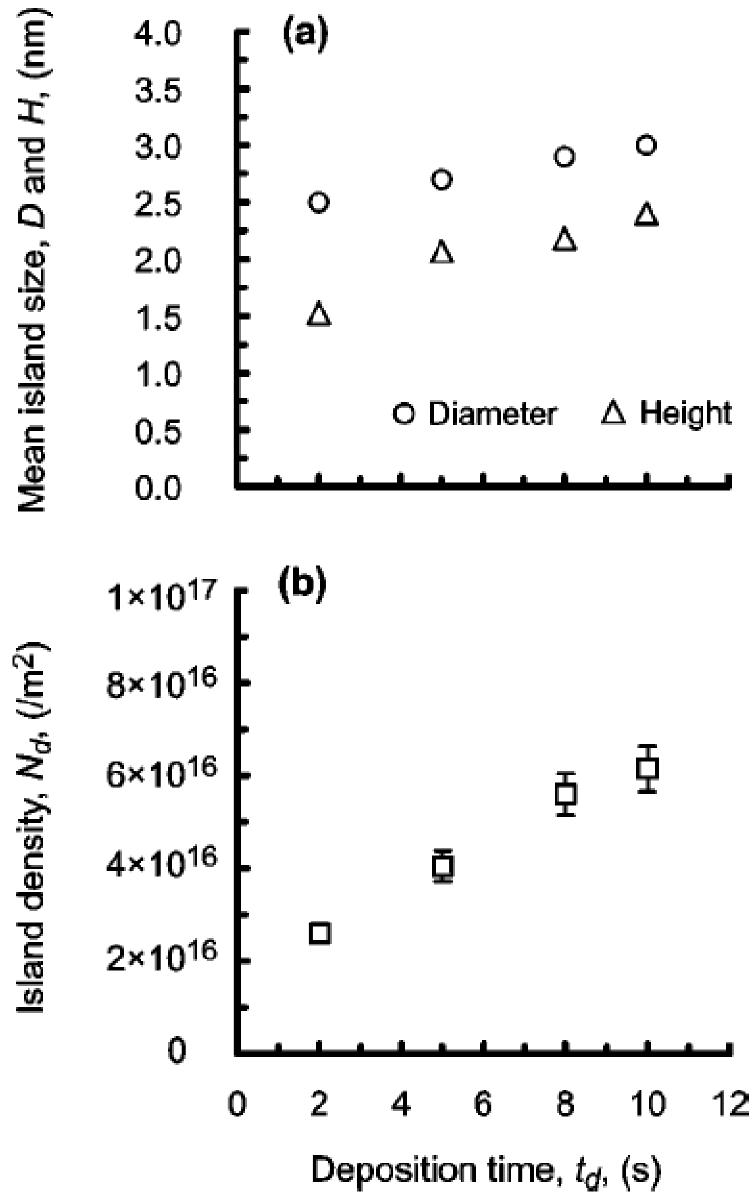

Fig. 8

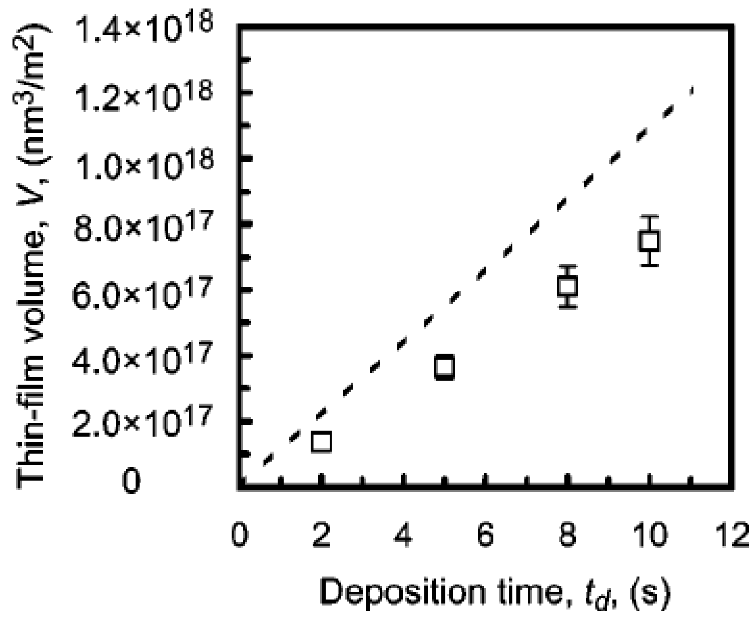

Fig. 9

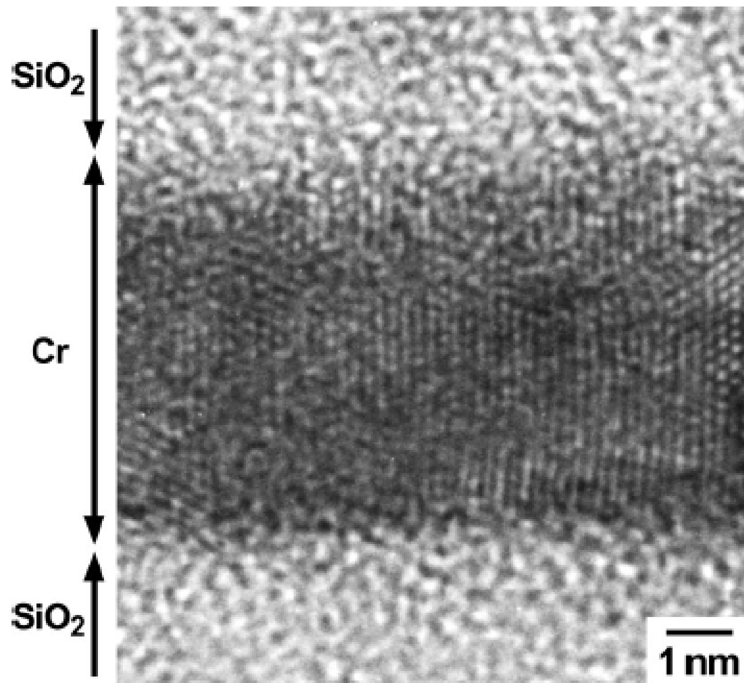

Fig. 10

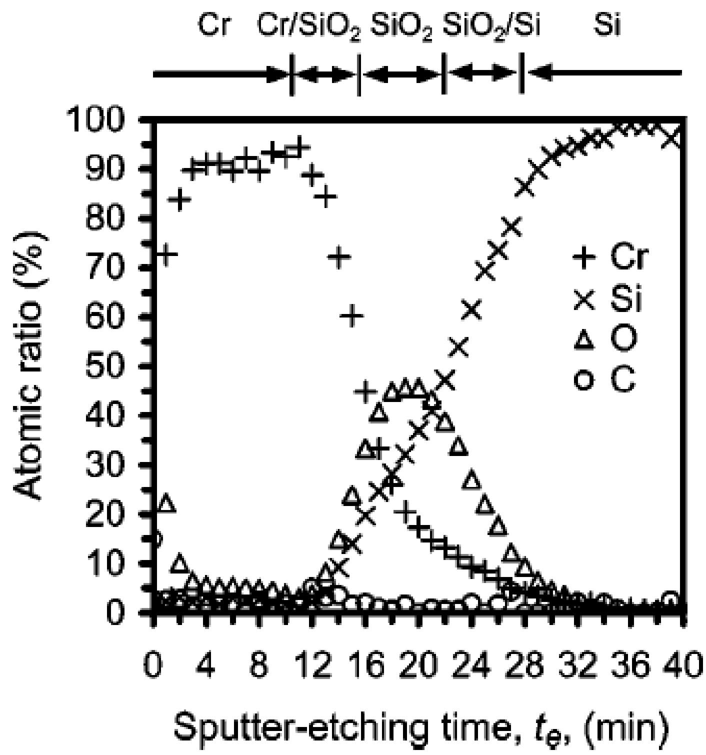

Fig. 11

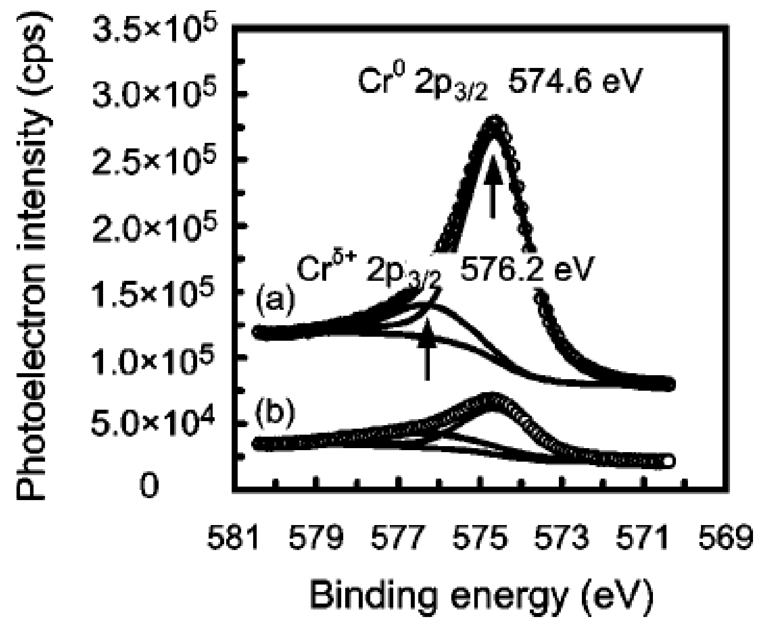

Fig. 12